$d_{01} = d_0 + d_1$, it is not the winner and is passed by. We then begin to test the next codevector. As the distance d_{01} is very small, we can determine the winner quickly.

Table 2: Comparison of performance of different codebook search methods

	Full search saving S	Method proposed in [3] saving S	Method proposed in this Letter saving S
	%	%	%
Real image at level 4 (codebook size: 1024, 4 dimensions, 9 bits per vector)	0	76.3	88.9
Real image at level 3 (codebook size: 1024, 4 dimensions, 9 bits per vector)	0	72.9	85.4
Real image at level 2 (codebook size: 512, 4 dimensions, 8 bits per vector)	0	70.5	79.6
Real image at level 1 (codebook size: 256, 4 dimensions)	0	68.3	78.9

Table 2 shows the results in terms of the percentage computational saving obtained over the full search method. It can be observed that use of the codebook searching method proposed in [3] can yield a 60–80% saving. However, if we utilise the special structure of TCVQ, we can reduce the computational complexity further.

Conclusion: We have presented a simple modified set partition method in order to maximise the minimum distance within subsets of a codebook and thus improve the TCVQ performance. The method can maximise the minimum distance within a subset for a small nonuniform distributed codebook. We have also proposed a computation acceleration scheme based on the partial distance search scheme and the codebook structure of TCVQ. This scheme can reduce the computational complexity by ~60–90%.

17 March 2000
Electronics Letters Online No: 20000643
DOI: 10.1049/el:20000643

Hu Mingyou and Tan Boon Tiong (*School of Electrical and Electronic Engineering, Nanyang Technological University, Nanyang Avenue, 639798, Singapore, Republic of Singapore*)

E-Mail: P146587283@ntu.edu.sg

References

1 WANG, H.S., and MOAYERI, N.: 'Trellis coded vector quantization', *IEEE Trans.*, 1992, **COM-40**, (8), pp. 1273–1276

2 FISCHER, T.R., and MARCELLIN, M.W.: 'Trellis coded vector quantization', *IEEE Trans.*, 1991, **IT-37**, (6), pp. 1551–1566

3 DA-BEI, C., and GRAY, R.M.: 'An improvement of the minimum distortion encoding algorithm for vector quantization', *IEEE Trans.*, 1985, **COM-33**, (10), pp. 1132–1133

4 MARCELLIN, M.W., and FISCHER, T.R.: 'Trellis coded quantization of memoryless and Gauss-Markov sources', *IEEE Trans.*, 1990, **COM-38**, (1), pp. 82–93

Determination of nonlinear coefficient n_2/A_{eff} using self-aligned interferometer and Faraday mirror

C. Vinegoni, M. Wegmuller and N. Gisin

A method for measuring the nonlinear coefficient n_2/A_{eff} in telecom fibres at 1550nm is presented. The method is based on determining the Kerr phase shift detected by a self-aligned interferometer incorporating a Faraday mirror. This makes the setup very robust, and different test fibres can be measured without the need for any further readjustments.

Introduction: The implementation of erbium-doped fibre amplifiers allows for high bit rate transmission over transoceanic distances. In addition the technique of wavelength division multiplexing (WDM) is used to increase the transmission rate, leading to a significant amount of power being inside the fibre. Because of the long distances and high powers, optical nonlinearities due to changes in the refractive index (optical Kerr effect) start to play a significant role. Among them, self-phase modulation (SPM), cross-phase modulation (XPM), and four-wave mixing (FWM) are the most important. The magnitudes of these effects depend on the ratio n_2/A_{eff}, where n_2 is the nonlinear refractive index of the fibre and A_{eff} the effective area of the lightmode. It is therefore important to have a simple and accurate method for determining this ratio. Different methods, based on SPM or XPM phase shift detection using interferometric and non-interferometric schemes have been proposed [1]. In this Letter, we present a different method based on the interferometric detection of a phase shift using a self-aligned interferometer with a Faraday mirror. This method has the advantages of being simple and all fibre implementable. Moreover, fluctuations due to environmental perturbations present in the other schemes mentioned above are avoided.

Principle of operation: The power dependence of the refractive index leads to a power dependent phase change ϕ of a pulse (peak power P, wavenumber k) travelling through a fibre of length L:

$$\phi(P) = \phi_1 + \phi_{n1} = n_0 kL + n_2 k L_{eff} \frac{P}{A_{eff}} m \qquad (1)$$

Fibre losses are accounted for by the effective length $L_{eff} = 1/\alpha [1 - \exp(-\alpha L)]$, with fibre loss coefficient α. The polarisation parameter m depends on the polarisation characteristics of the test fibre and the signal polarisation state. It is equal to 1 for the case of a polarisation maintaining fibre if the light is coupled into one of the two axes [2], whereas for a sufficiently long standard telecom fibre with a complete scrambling of the polarisation, it was demonstrated that $m = 8/9$ [3]. Using eqn. 1, measurement of the acquired phase shift will enable the ratio n_2/A_{eff} to be determined or, through an independent measurement of A_{eff}, the value of n_2.

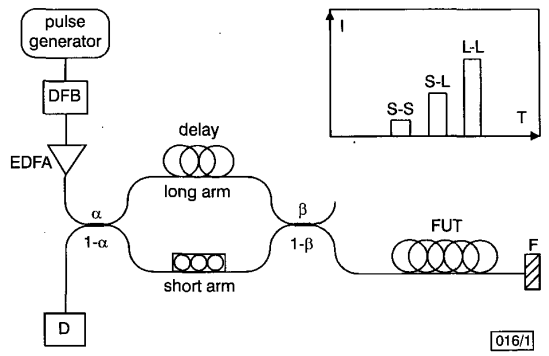

Fig. 1 *Experimental setup of self-aligned interferometer*

DFB: distributed feedback laser; EDFA: erbium doped fibre amplifier; PC: polarisation controller; FUT: fibre under test; FM: Faraday mirror; D: detector

The phase shift is measured using the self-aligned interferometer shown in Fig. 1. Amplified laser pulses are split at the first coupler (coupling ratio $\alpha/(1 - \alpha)$). They then move along the two

interferometer arms, which are different in length so that the two pulses do not interfere on recombination at the second coupler (coupling ratio $\beta/(1-\beta)$). One of the exit arms of this last coupler is connected to the fibre under test (FUT) of which n_2/A_{eff} is to be measured. For an adequate choice of α and β, the two pulses in the FUT strongly vary in power, and consequently experience (according to eqn. 1) a different degree of phase shift. After being reflected at the Faraday mirror (FM) [4, 5], the pulses return back through the FUT towards the first coupler.

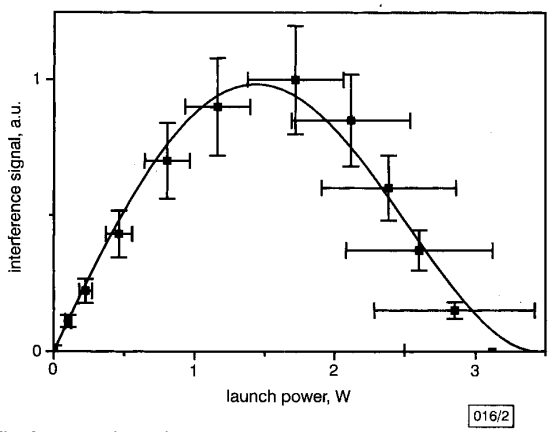

Fig. 2 *Detected interference signal power against launch power*
■ measured
——— theoretical fit

Four different trajectories through the interferometer are possible during the forward and return path: a double pass of the long-arm (long-long), of the short-arm (short-short), and a forward pass of the short (long) arm with a return pass through the opposite arm (short-long and long-short, respectively). Owing to the differences in path length, three different arrival times at the detector can be discerned, as is schematically shown in the inset of Fig. 1. Only the middle pulse, which is due to the interference between the short-long and long-short pulses, is interesting and will be further analysed. Its power at the detector depends on the phase relationship between the two interfering signals, and it can therefore be exploited to calculate the nonlinear phase shift experienced in the FUT. Note that contrary to regular Mach-Zehnder interferometers, the balancing of the interferometer arms is not critical as the path lengths of the two interfering signals are automatically matched (self-aligned).

Obviously, the power of this middle pulse also depends on the polarisation states of the two interfering signals, given by

$$|\psi_{LS}\rangle = R_S^{-1}(R_{FUT}^{-1}FR_{FUT})R_L|\psi_0\rangle = R_S^{-1}FR_L|\psi_0\rangle \equiv A|\psi_0\rangle$$
$$|\psi_{SL}\rangle = R_L^{-1}(R_{FUT}^{-1}FR_{FUT})R_S|\psi_0\rangle = R_L^{-1}FR_S|\psi_0\rangle \equiv B|\psi_0\rangle \quad (2)$$

for the long-short and short-long path, respectively. $|\Psi_0\rangle$ is the input state of polarisation, and R_L, R_S, $RFUT$, and F are the transformation operators for the long arm and short arm, the FUT, and the FM, respectively. The use of an FM as a reflector removes polarisation transformations of the FUT, thereby fixing its output polarisation. Note that using a standard mirror in place of the FM, an additional PC would be required, which not only makes the initial adjustments difficult, but also leads to an undesired FUT dependence. For optimum visibility, full interference is required between the two signals, i.e. $A = B$ in eqn. 2, which can be obtained by properly adjusting the PC such that $R_L = R_S$. In practice, this is achieved by setting the PC so that the output intensity is maximised for low input pulse power and with the FM directly connected to the interferometer (i.e. no FUT and therefore no nonlinear phase shift is present). This setting can then be used throughout the measurements, without the need for readjustments as long as there is no significant change in R_L or R_S. Note that the fact that the bias of our interferometer can be adjusted is due to a geometrical phase (Pancharatnam-effect, [6]): at the PC, the clockwise travelling pulse has experienced a π phase shift (with respect to the anti-clockwise travelling pulse) from the FM reflection. Using the described adjustment, the detected power becomes proportional to

$$P_{out}(P) \propto P\cos^2(\Delta\phi) \quad (3)$$

where $\Delta\phi$ is the amount of nonlinear phase shift, equal to

$$\Delta\phi(P) = \frac{2\pi}{\lambda}PL_{eff}(\alpha-\beta)m\frac{n_2}{A_{eff}} \quad (4)$$

Straightforward calculation shows that for maximum visibility of the detected signal, one of the two couplers has to be symmetric (50/50). To obtain a good accuracy for n_2/A_{eff}, the measurements are carried out for different launch powers P. Ideally, the length of the FUT is long enough to allow for good polarisation scrambling and to be able to detect the first zero pass at $\Delta\phi = \pi/2$ for the available launch power.

Results and discussion: For the practical implementation of the above concept, we used a directly modulated DFB laser diode with a wavelength of 1559nm and consecutive amplification by an EDFA. The pulse duration was 28ns with a repetition rate of 1kHz. Note that in some fibres, such pulses can excite acoustic waves through electrostriction, leading to erroneous n_2/A_{eff} values: a laser source with shorter pulses should be used to avoid this risk. For the couplers, a 50/50 ratio was used for the first one and a 90/10 for the second.

Fig. 2 displays the magnitude of the interference signal as a function of the launch power P for a standard telecom fibre (SMF) with a length of 1100 m used as the FUT. The experimentally obtained values (squares) are fitted using eqn. 3. The data correspond well with the model ($\chi^2 = 3 \times 10^{-3}$). As can be seen, the signal slowly increases reaching a maximum value at 1.4W. For higher powers the nonlinear phase shift becomes more important and the signal decreases reaching a null value at 3.4W corresponding to a full $\pi/2$ phase shift. From the fit we obtain a value of $(2.76 \pm 0.04)\ 10^{-10}\text{W}^{-1}$ for the nonlinear coefficient n_2/A_{eff}. Having found with the refracted-near-field method [7] a value of $(88 \pm 3)\ \mu\text{m}^2$ for A_{eff}, the nonlinear refractive index n_2 becomes $(2.4 \pm 0.1)\ 10^{-20}$ m^2/W.

Conclusion: We have described a simple method for the measurement of the nonlinear coefficient n_2/A_{eff} based on an all fibre, self-aligned interferometer. The self-alignment characteristic not only allows for an easy and quick initial adjustment of the interferometer, but along with the use of a Faraday mirror also makes it robust against environmental perturbations. This leads to good accuracy for the measured n_2/A_{eff} values. The proposed method is well suited to the routine measurement of the nonlinear coefficient because, owing to the presence of the FM, the fibre under test can be easily exchanged without necessitating any further readjustments of the interferometer.

Acknowledgments: We acknowledge the financial support from the Swiss Federal Office for Education and Sciences (OFES) in the framework of the European COST 265 programme.

24 March 2000
Electronics Letters Online No: 20000668
DOI: 10.1049/el:20000668

C. Vinegoni, M. Wegmuller and N. Gisin (*Group of Applied Physics, University of Geneva, 20 École-de-Mèdecine, CH-1211, Geneva 4, Switzerland*)

E-mail: claudio.vinegoni@physics.unige.ch

References

1 FELLEGARA, A., ARTIGLIA, M., ANDREASEN, S.B., MELLONI, A., ESPUNES, F.P., and WABNITZ, S.: 'COST 241 intercomparison of nonlinear refractive index measurements in dispersion shifted optical fibres at λ = 1550nm', *Electron. Lett.*, 1997, **33**, pp. 1168–1170

2 WITTL, F., VOBIAN, J., HERCHENROEDER, G., and DULTZ, W.: 'Interferometric determination of the nonlinear refractive index n_2 of optical fibers'. Tech. Dig. Symp. Optical Fiber Measurements, 1996, pp. 71–74 (NIST SP 905)

3 CHERNIKOV, S.V., and TAYLOR, J.R.: 'Measurement of normalization factor of n_2 for random polarization in optical fibers', *Opt. Lett.*, 1996, **21**, (19), pp. 1559–1561
4 MARTINELLI, M.: 'A universal compensator for polarization changes induced by birefringence on a retracing beam', *Opt. Commun.*, 1989, **72**, pp. 341–344
5 BREGUET, J., PELLAUX, J.P., and GISIN, N.: 'Photoacoustic detection of trace gases with an optical microphone', *Sens. Actuators AV*, 1995, **1**, pp. 29–35
6 PANCHARATNAM, S.: 'Collected works of S. Pancharatnam' (Oxford University Press, London, 1975)
7 GISIN, N., PASSY, R., and PERNY, B.: 'Optical fiber characterization by simultaneous measurement of the transmitted and refracted near field', *J. Lightwave Technol.*, 1993, **11**, pp. 1875–1883

GSM/FEM modelling of plane wave scattering from photonic crystals with defects

A. Freni and C. Mias

A hybrid generalised scattering matrix (GSM)/finite element method (FEM) formulation is proposed for modelling the effect of the presence of defects in photonic crystals. It is employed to analyse uniform slab and periodic defects in a triangular-lattice structure consisting of dielectric cylinders.

Introduction: The finite element method has been widely used in the modelling of periodic structures of both two and three dimensional profiles [1]. Its advantage is the ease with which periodic structures of complex geometry can be modelled [2]. As the complexity of the structure and its size with respect to wavelength increase, the number of finite elements also increases, necessitating an increase in computational resources (memory and time). This problem becomes particularly acute when analysing photonic bandgap (PBG) structures [3] which are stacks of periodic layers that may include defects. To overcome the problem, a hybrid generalised scattering matrix (GSM)/finite element method (FEM) formulation is proposed. Following this method, the unit cell of each periodic layer is split into a stack of thinner sections. The scattering matrix of each section in the stack (different sections may have different geometries) is evaluated by employing a hybrid finite element/boundary element (FE/BE) formulation [2]. The scattering matrices are then combined appropriately. The periodic layers need not have the same period, i.e. multiple periods can also be considered. This multiplicity can be exploited to reduce further the computational time requirements.

Formulation: Fig. 1 shows a PBG structure. It consists of a finite number of periodic layers along the x direction. Along the y direction, each defectless layer is infinitely periodic with period $\tilde{D}_y$ (Fig. 2*b*). The only restriction in the present method is that the layers with defects must be periodic with period D_y which is an integer multiple of $\tilde{D}_y$ (i.e. $D_y = M\tilde{D}_y$ with $M = 1, 2, ...$). The generic ith section, Fig. 2*b* or *c*, is delimited by an upper and lower plane, $\Gamma^{(i)}$ and $\Gamma^{(i+1)}$, respectively. It is assumed that the medium surrounding it is free space. The incident plane wave is independent of the z co-ordinate and has an electric field parallel to the z-axis (TM_z polarisation, $H_z = 0$). The GSM/FEM analysis procedure for the TE_z case (i.e. $E_z = 0$) is similar and thus this polarisation is not considered. A harmonic time dependence $e^{j\omega t}$ is assumed and suppressed. Since the complete structure is periodic with period D_y, only a unit periodic cell (such as that shown in Fig. 2*c*) is considered in which $-D_y/2 \le y \le D_y/2$. By invoking Floquet's theorem the field at the generic boundary $\Gamma^{(i)}$ can be represented by a summation of an infinite number of spatial harmonics which are plane waves [4]:

$$E_z^{(i)} = \sum_{n=-\infty}^{+\infty} \left(V_{+,n}^{(i)} \exp\left(-jk_{x,n}^{(i)}x\right) + V_{-,n}^{(i)} \exp\left(+jk_{x,n}^{(i)}x\right)\right) \times \exp(-jk_{y,n}y) \quad (1)$$

with $k_{y,n} = k_y^{inc} + 2\pi n/D_y$, $k_{x,n}^{(i)} = \sqrt{[(k^{(i)})^2 - k_{y,n}^2]}$, $Im(k_{x,n}^{(i)}) < 0$, where n is the harmonic order, $k_y^{inc} = k_0 \sin\phi^{inc}$ and $k^{(i)} = \omega\sqrt{[\varepsilon_i\mu_i]}$ is the propagation constant of the uniform medium where the boundary $\Gamma^{(i)}$ is located. In the computations, the number of harmonics is truncated appropriately, $n \in [-N, N]$. The +/– subscripts indicate wave propagation in the positive/negative x direction, respectively.

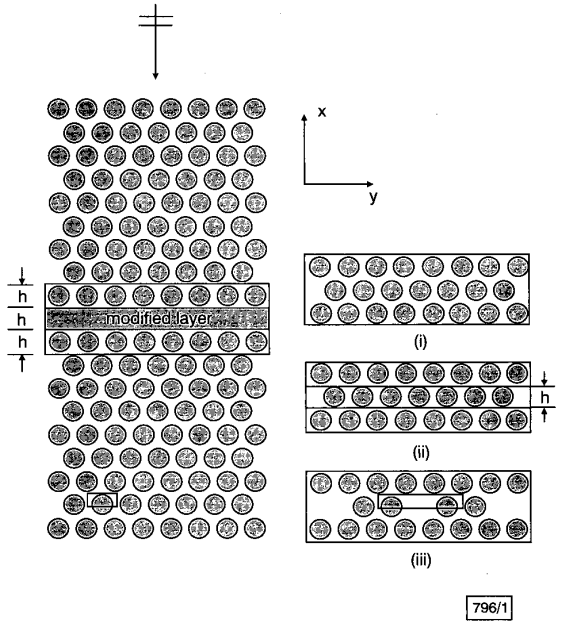

Fig. 1 *Geometry of structure*

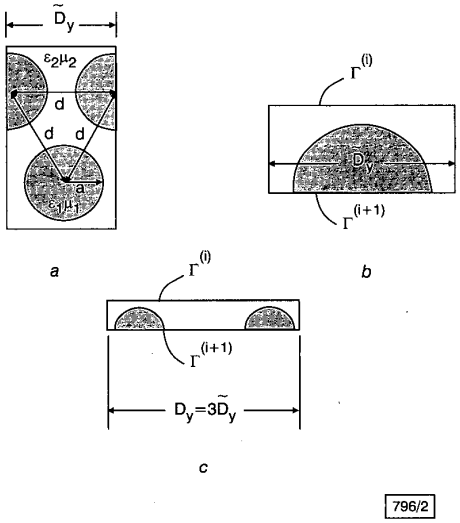

Fig. 2 *Structure characteristics, periodic call for modified layer, and periodic cell for layers above and below modified layer*

a Structure characteristics
b Periodic cell for layers above and below modified layer
c Periodic cell for modified layer (iii)

The harmonics are orthogonal functions, thus for each section i we can define a column vector $\mathbf{a}^{(i)} = [\mathbf{V}_-^{(i)}\ \mathbf{V}_+^{(i+1)}]^T$ of the amplitudes of the incident waves and a column vector $\mathbf{b}^{(i)} = [\mathbf{V}_+^{(i)}\ \mathbf{V}_-^{(i+1)}]^T$ of the amplitudes of the scattered waves, where $\mathbf{V}_\pm^{(i)} = [V_{\pm,-N}^{(i)}\ V_{\pm,-(N-1)}^{(i)} \dots V_{\pm,N}^{(i)}]$. The above definition allows the stacked sections to be represented as a cascade of multiport devices. The generalised scattering matrix of the ith section is created by considering each harmonic n as the incident plane wave and evaluating the scattered harmonic amplitudes via the FE/BE method [2]. Subsequently, efficient connection schemes are applied to compute the total generalised scattering matrix of the whole stack and thus evaluate the reflected and transmitted harmonic powers.

The computational effort can be reduced when considering layers that have a period which is an integer fraction of the